



## ORIGINAL ARTICLE

# Self-compacting microconcretes containing ornamental stone waste and expanded polystyrene residue: influence of the ratios filler/cement and lightweight /conventional aggregates

*Microconcretos autoadensáveis contendo resíduo de rocha ornamental e resíduo de poliestireno expandido: influência das relações filler/cimento e agregados leves/convencionais*

Ariel Miranda de Souza<sup>a</sup>

José Maria Franco de Carvalho<sup>a</sup>

Carol Ferreira Rezende Santos<sup>a</sup>

Flávio Antônio Ferreira<sup>a</sup>

Leonardo Gonçalves Pedroti<sup>a</sup>

Ricardo André Fiorotti Peixoto<sup>b</sup>

<sup>a</sup>Universidade Federal de Viçosa – UFV, Departamento de Engenharia Civil, Viçosa, MG, Brasil

<sup>b</sup>Universidade Federal de Ouro Preto – UFOP, Departamento de Engenharia Civil, Ouro Preto, MG, Brasil

Received 22 February 2023

Revised 13 July 2023

Accepted 22 December 2023

Corrected 27 March 2024

**Abstract:** Eco-efficient self-compacting micro concretes with partial replacement of Portland cement by ornamental stone waste (OSW) and replacement of conventional aggregates by expanded polystyrene waste were addressed in this study. A base mixture was obtained using a particle packing method, and replacement fractions followed a second-order composite experimental design. The mixtures' rheological, physical, mechanical and eco-efficiency parameters were evaluated and discussed. As expected, the incorporation of residues reduced the mechanical strength, and mixtures with high incorporation of lightweight aggregates tended to segregate. However, OSW has been shown to increase workability and decrease viscosity, contributing to control segregation due to the reduced amount of water required without impairing the fluidity of the mix. At the same time, the lightweight aggregate decreased both the density of the mixtures and the viscosity. The interaction of the residue with the lightweight aggregate proved promising in obtaining more eco-efficient lightweight microconcretes.

**Keywords:** lightweight concrete, self-compacting concrete, microconcrete, ornamental stone waste, expanded polystyrene waste, lightweight aggregate.

**Resumo:** Foram abordados neste estudo micro concretos autoadensáveis ecoeficientes com substituição parcial do cimento Portland por resíduo de rochas ornamentais (do inglês ornamental stone waste - OSW) e substituição dos agregados convencionais por resíduo de poliestireno expandido. A dosagem foi feita utilizando metodologia de empacotamento de partículas, e as frações de substituição seguiram um projeto experimental estatístico composto de segunda ordem. Foram avaliados e discutidos os parâmetros reológicos, físicos, mecânicos e de ecoeficiência das misturas. Como esperado, a incorporação dos resíduos diminuiu a resistência mecânica, e as misturas com elevadas incorporações de agregados leves apresentaram tendência a segregação. Entretanto, a adição do resíduo OSW demonstrou aumentar a trabalhabilidade e diminuir a viscosidade, contribuindo para controlar a segregação devido à redução no consumo de água necessário sem prejudicar a fluidez da mistura. Ao mesmo tempo, o agregado leve diminuiu tanto a densidade das misturas quanto a viscosidade. A interação do resíduo com o agregado leve se mostrou promissora na obtenção de microconcretos leves mais ecoeficientes.

**Palavras-chave:** concreto leve, concreto autoadensável, micro concreto, resíduo de rocha ornamental, resíduo de poliestireno expandido, agregado leve.

**How to cite:** A. Miranda de Souza, J. M. Franco de Carvalho, C. F. R. Santos, F. A. Ferreira, L. G. Pedroti, and R. A. F. Peixoto, "Self-compacting microconcretes containing ornamental stone waste and expanded polystyrene residue: influence of the ratios filler/cement and lightweight /conventional aggregates," *Rev. IBRACON Estrut. Mater.*, vol. 17, no. 6, e17605, 2024, <https://doi.org/10.1590/S1983-41952024000600005>.

**Corresponding author:** Ariel Miranda de Souza. E-mail: ariel.souza@ufv.br

**Financial support:** This study was financed in part by the Coordenação de Aperfeiçoamento de Pessoal de Nível Superior – Brasil (CAPES) – Finance code 001, Fundação de Amparo à Pesquisa do Estado de Minas Gerais (FAPEMIG) – highlighting the project APQ-02637-21, and Conselho Nacional de Desenvolvimento Científico e Tecnológico (CNPq).

**Conflict of interest:** The authors declare that they have no conflict of interest.

**Data Availability:** the data that support the findings of this study are available from the corresponding author, A. Miranda de Souza, upon reasonable request.

This document has an erratum: <https://doi.org/10.1590/S1983-41952024000600016>



This is an Open Access article distributed under the terms of the Creative Commons Attribution License, which permits unrestricted use, distribution, and reproduction in any medium, provided the original work is properly cited.

## 1 INTRODUCTION

Lightweight aggregates self-compacting concrete (LWASCC) have been studied for structural and non-structural purposes in slender pieces with high reinforcement rates to reduce weight and obtain a more fluid mixture [1]–[3]. Researches involving lightweight aggregates (LWA), natural or artificial, have been carried out to understand their behavior in cement matrices, reducing density from 2400 kg/m<sup>3</sup> to values below 2000 kg/m<sup>3</sup> [4]–[9].

Reducing specific mass while maintaining the mechanical strength permits lighter structural elements, reducing the loads transferred to the foundation and saving costs for using lighter lifting equipment [1], [2], [10], [11]. In addition, such a solution contributes to driving the growth of sustainable building construction, soundproof and thermally insulating green buildings using low-density and low-cost materials [2].

However, the low density of LWA leads to a reduction in the mechanical strength of LWASCC, making a large volume of cement necessary to ensure structural strength, which implies low environmental efficiency due to the high energy-demanding cement production, which accounts for around 7% of the global emissions of carbon dioxide (CO<sub>2</sub>) [12]–[19].

Segregation and exudation can occur in fresh self-compacting concrete containing LWA due to the lower density of the aggregates compared to the other components, favoring the float of the aggregates and absorption of the mixing water and admixtures, making it difficult to spread and self-consolidate the mixture, resulting in loss of mechanical strength [1], [3], [6]–[8]. Segregation can be overcome by adjusting cohesion and consistency in a higher yield strength paste, which can be achieved by controlling the water/cement ratio and using mineral and rheology-modifying admixtures [1], [3], [8].

Fillers effectively increase cohesion and prevent segregation and flotation of lightweight aggregates for low-density self-compacting concretes [1], [20]–[23]. A material prone to being used as a filler is ornamental stone waste (OSW), which has a fine granulometry. This material is produced in high volumes annually and is eligible for use in civil construction [24]–[26].

Studies in the literature addressing OSW in lightweight concrete are scarce. Zafar et al. [27] studied the use of granite residue in autoclaved concrete as a substitute for sand and observed a low pozzolanic action but an increase in the packing density of the mixtures, concrete density, mechanical strength, strong acid resistance, and a decrease in porosity and absorption. Alyousef et al. [28] studied the replacement of sand with marble residue in lightweight concrete floor blocks containing expanded perlite and verified an increase in concrete density and strength and the possibility of being used as insulation blocks.

From the authors' knowledge, incorporating OSW into lightweight aggregate self-compacting microconcrete (without coarse aggregate) has not been addressed in the literature. Thus, this study aimed to investigate the effects of partial replacement of Portland cement by OSW in lightweight self-compacting microconcretes containing expanded polystyrene residue as lightweight aggregate. Physical, mechanical and environmental parameters have been evaluated and discussed in an approach involving cement consumption and contributions to producing a more sustainable material.

## 2 EXPERIMENTAL

### 2.1 Materials

Expanded polystyrene waste provided by a company located in the city of São Geraldo, Minas Gerais State, Brazil, was used as lightweight aggregate (LWA). The Ornamental Stone Waste (OSW) filler was provided by a manufacturer in Cachoeiro de Itapemirim, Espírito Santo, Brazil. A high early-strength Portland cement (PC) (type IV equivalent, designated in Brazil as CPV-ARI) was used as a binder. Two conventional aggregates were used: natural quartz river sand (R-Sand) and manufactured gneiss sand (M-Sand), both from the region of Viçosa, Minas Gerais, Brazil. A commercial superplasticizer based on polycarboxylate ether (PCE) was used as a water reducer. Tables 1 to 3 present the physical properties of cement and OSW, the chemical properties of OSW, and the physical properties of the aggregates, respectively. Figure 1 shows the particle size distribution curves of the materials, Figure 2 shows an image of the LWA, Figure 3 shows the scanning electron microscope (SEM) images of OSW, and Figure 4 shows the XRD spectra of OSW.

According to the XRD analysis of the OSW sample, the presence of quartz and dolomite may indicate a mixture of granite and marble residues. This material also has a regular and crystalline surface, which leads to low reactivity and pozzolanicity and can be considered inert.

**Table 1.** Physical properties of the Portland Cement (PC) and ornamental stone waste (OSW).

| Material         | Specific density (g/cm <sup>3</sup> ) | Specific surface area (Blaine) (cm <sup>2</sup> /g) |
|------------------|---------------------------------------|---|
| PC               | 3.15                                  | 2135.81   |
| OSW              | 2.60                                  | 2996.11   |
| M-sand           | 2.86                                  | -   |
| R-sand           | 2.63                                  | -   |
| Superplasticizer | 1.09                                  | -   |

**Table 2.** Chemical composition of the ornamental stone waste (OSW).

| Compound                                  | OSW  |
|---|------|
| SiO <sub>2</sub> content. %               | 74.5 |
| CO <sub>2</sub> content. %                | 8.1  |
| Al <sub>2</sub> O <sub>3</sub> content. % | 5.3  |
| CaO content. %                            | 5.0  |
| MgO content. %                            | 3.5  |
| Na <sub>2</sub> O content. %              | 1.7  |
| K <sub>2</sub> O content. %               | 1.0  |
| Fe <sub>2</sub> O <sub>3</sub> content. % | 0.6  |
| TiO <sub>2</sub> content. %               | 0.1  |
| Other oxides. %                           | 0.1  |

**Table 3.** Physical properties of the manufactured gneiss sand (M-Sand), river sand (R-Sand) and lightweight aggregate (LWA).

| Material | Bulk density (g/cm <sup>3</sup> ) |
|----------|-----------------------------------|
| M-Sand   | 1.56E+00                          |
| R-Sand   | 1.43E+00                          |
| LWA      | 5.21E-03                          |

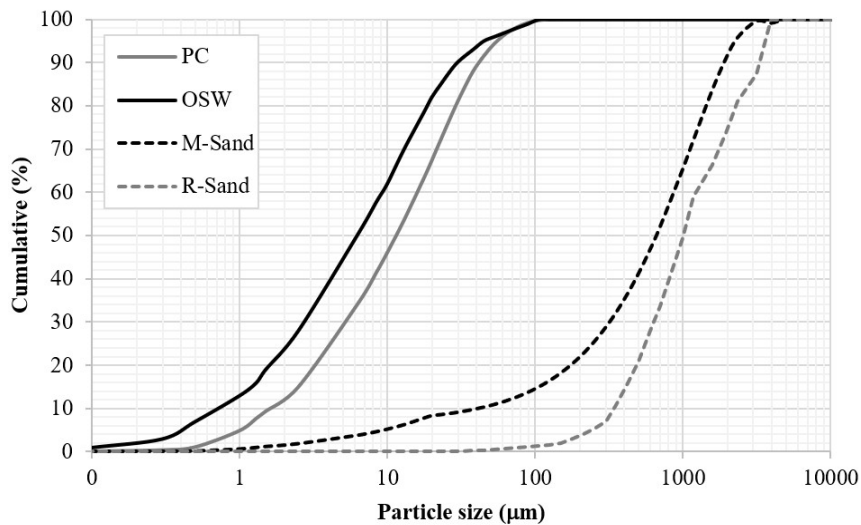


**Figure 1.** Granulometric curves of the Portland Cement (PC), ornamental stone waste (OSW), manufactured gneiss sand (M-Sand), and river sand (R-Sand).



Figure 2. EPS waste used as lightweight aggregate.

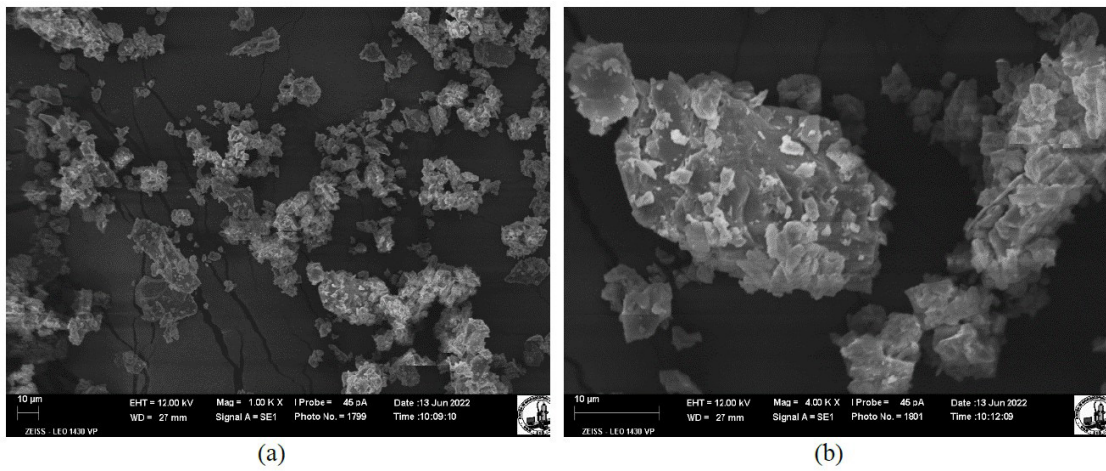


Figure 3. Scanning electron microscope (SEM) images of OSW in (a) 1.00kx and (b) 4.00kx magnification.

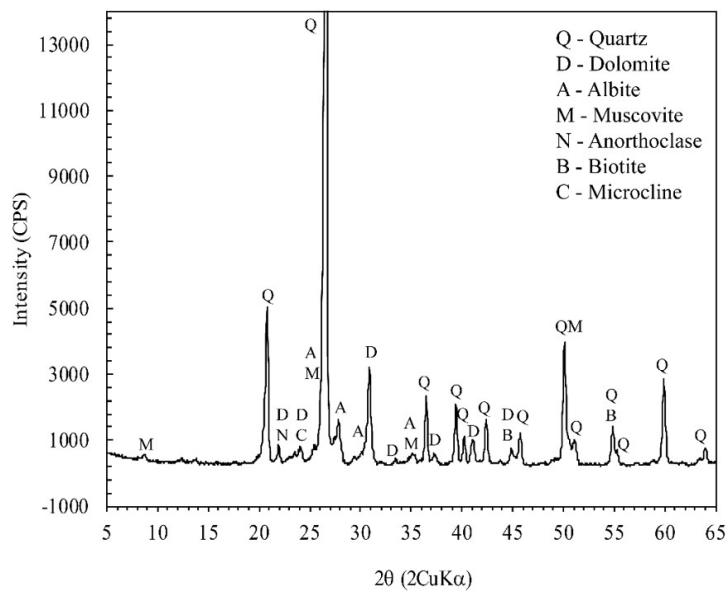


Figure 4. XRD spectra of ornamental stone waste (OSW).

## 2.2 Experimental design

The reference mixture was designed by fitting the particle size distribution curve of a blend of constituents to the modified Andreassen packing curve [29], obtained using Equation 1, where  $CPFT$  is the accumulated percentage of particles with a diameter smaller than  $D$  (by volume);  $D$  is the particle size;  $D_L$  is the diameter of the largest particle;  $D_S$  is the diameter of the smallest particle; and  $q$  is the distribution coefficient ( $q$ -value).

$$CPTF (\%) = 100 \left( \frac{D^q - D_S^q}{D_L^q - D_S^q} \right) \tag{1}$$

The powder and aggregate contents were obtained by fitting the modified Andreassen curve and simultaneously meeting the limits suggested by EFNARC [20]. For this, the distribution coefficient should be between 0.20 and 0.23; then, 0.2 was used to provide a higher content of fines, increasing the mixture's viscosity, maintaining workability, and reducing the tendency to segregate the lightweight aggregates [30]–[34].

The modified Andreassen curve adjustment data established a proportion of sands of 1:3 (R-Sand/M-Sand) and a powder-to-total solid volume ratio ( $V_p/V_t$ ) of 35%. Once the reference dosage was established by the compressible packing method and the limits of the experimental method, the statistical factorial model methodology was used to define the volume ratios filler/cement ( $f/c$ ) and lightweight/conventional aggregates ( $V_{LWA}/V_{CA}$ ) in order to reduce the number of samples to be tested and to obtain results adjusted by statistical equations [19].

Filler-to-cement ( $f/c$ ) ratios between 0 and 200% and  $V_{LWA}/V_{CA}$  between 0% and 60% were used as limits for the experimental design. For the calculations of  $V_{LWA}/V_{CA}$ , bulk density was used as converting parameter due to the low specific density of the residue and the difficulty of measuring it.

The proportions of the mixtures were defined following a second-order composite project (as illustrated in Figure 5 and presented in Table 4). The proportions of the mixtures by volume of dry materials and the consumptions in mass are presented in Table 5. The mixtures were named according to the  $f/c$  and  $V_{LWA}/V_{CA}$  ratios in percentage (e.g., 170F51LWA has 1.7  $f/c$  and 0.51  $V_{LWA}/V_{CA}$ ).

The water/powder ( $V_w/V_p$ ) ratio was adjusted to a spread of  $270 \pm 10$  mm in a mini-slump test to obtain mixtures that did not show apparent exudation and segregation. The superplasticizer content was set at 1% of the mass of the total powder content. The superplasticizer was added and accounted into the mixing water.

The mini-slump test was adapted using a cone 75 mm high with diameters of 41 mm and 91 mm. The results were compared through the fluidity parameter  $G_m$  obtained by Equation 2 proposed by Okamura and Ouchi [23], where  $D_m$  is the spreading diameter, and  $D_0$  is the inner diameter of the base of the cone [20], [21].

$$G_m = \left( \frac{D_m}{D_0} \right)^2 - 1 \tag{2}$$

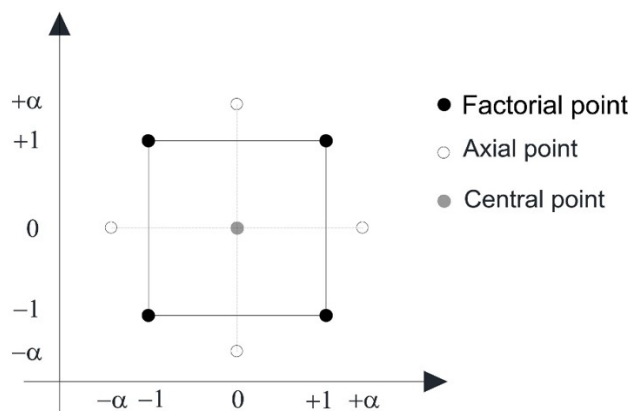


Figure 5. Second-order composite project.

**Table 4.** Levels of variables used in LWASCC.

| Proportions  | -1.41 | -1   | 0    | 1    | 1.41 |
|--|-------|------|------|------|------|
| Filler/cement (f/c)                                      | 0.00  | 0.29 | 1.00 | 1.71 | 2.00 |
| Lightweight/conventional aggregates ( $V_{LWA}/V_{CA}$ ) | 0.00  | 0.09 | 0.30 | 0.51 | 0.60 |

**Table 5.** Mixtures of LWASCM (PC - Portland Cement; OSW - ornamental stone waste; M-Sand - artificial sand; R-Sand - river sand; LWA - lightweight aggregate; W- water; SP - superplasticizer).

| Mixture                     | 100F<br>0LWA | 170F<br>9LWA | 29F<br>9LWA | 0F<br>30LWA | 100F<br>30LWA | 200F<br>30LWA | 170F<br>51LWA | 29F<br>51LWA | 100F<br>60LWA |
|-----------------------------|--------------|--------------|-------------|-------------|---------------|---------------|---------------|--------------|---------------|
| f/c                         | 0            | 1            | -1          | -1.4142     | 0             | 1.4142        | 1             | -1           | 0             |
| $V_{LWA}/V_{CA}$            | -1.4142      | -1           | -1          | 0           | 0             | 0             | 1             | 1            | 1.4142        |
| PC (%)                      | 20           | 14.78        | 30.94       | 40          | 20            | 13.33         | 14.78         | 30.94        | 20            |
| OSW (%)                     | 20           | 25.22        | 9.06        | 0           | 20            | 26.67         | 25.22         | 9.06         | 20            |
| M-Sand (%)                  | 45           | 41.05        | 41.05       | 31.5        | 31.5          | 31.5          | 21.95         | 21.95        | 18            |
| R-Sand (%)                  | 15           | 13.68        | 13.68       | 10.5        | 10.5          | 10.5          | 7.32          | 7.32         | 6             |
| LWA (%)                     | 0            | 5.27         | 5.27        | 18          | 18            | 18            | 30.73         | 30.73        | 36            |
| PC (kg/m <sup>3</sup> )     | 462.41       | 335.42       | 671.83      | 832.44      | 449.93        | 317.07        | 338.5         | 666.04       | 462.41        |
| OSW (kg/m <sup>3</sup> )    | 391.27       | 484.51       | 166.5       | 0           | 380.71        | 536.59        | 488.95        | 165.06       | 391.27        |
| M-Sand (kg/m <sup>3</sup> ) | 953.61       | 854.02       | 816.93      | 600.84      | 649.51        | 686.57        | 460.97        | 433.18       | 381.44        |
| R-Sand (kg/m <sup>3</sup> ) | 291.76       | 261.29       | 249.94      | 183.83      | 198.72        | 210.06        | 141.03        | 132.53       | 116.7         |
| LWA (kg/m <sup>3</sup> )    | 0            | 0.37         | 0.35        | 1.15        | 1.24          | 1.31          | 2.16          | 2.03         | 2.56          |
| W (kg/m <sup>3</sup> )      | 258.95       | 272.41       | 304.01      | 332.98      | 278.96        | 237.8         | 265.74        | 310          | 258.95        |
| SP (kg/m <sup>3</sup> )     | 9.25         | 9.08         | 8.69        | 8.32        | 9             | 9.51          | 9.16          | 8.61         | 9.25          |

### 2.3 Concrete production and specimens casting

The LWASCM were prepared using a Philco PHP500 planetary mixer according to the following protocol: (a) the dry mix was homogenized; (b) the initial kneading water containing all the superplasticizer was added to the homogenized dry mixture, with the mixer at slow speed, over 30 seconds; (c) the mixer was kept at slow speed for additional 60 seconds before being (d) turned off to clean the blades and bowl walls, keeping the mixture at rest for 60 seconds; in sequence (e) the mixer was restarted, and the mixture was homogenized for an additional time of 60 seconds at medium speed.

The volume of mixed material was 1770±10 mL, enough to mold 9 cylindrical test specimens measuring Ø5×10 cm. The specimens were demolded at 1 day of age and kept submerged in lime-saturated water for curing.

### 2.4 Rheological tests

In the fresh state, spreading and tendency to segregation and exudation were analyzed using the adapted mini-slump test. The viscosity was measured through the time ( $T_{220}$ ) that the mixture takes to reach a spread with a diameter equal to 220 mm. In addition, the results were compared to the viscosities of pastes with f/c ratios of 0, 1 and 2, water/power ratio of 1.5 and superplasticizer content of 3%, measured using a FANN 35A rotational viscometer.

### 2.5 Concrete characterization test

The mechanical, chemical and physical characterization tests were conducted in the hardened state. The tensile strength test by diametrical compression and compressive strength test in cylindrical specimens (Ø5×10 cm) were carried out following the methods NBR 7222 [35], NBR 5739 [36] and ASTM C-39 [37]. The dynamic modulus of elasticity and setting time of the LWASCM were also determined by measuring the ultrasonic pulse velocity (UPV) (Proceq Pundit Lab, P wave, frequency 54 kHz) according to the NBR 8802 [38] and ASTM C597-16 [39].

For the physical characterization in the hardened state, specific density and void index tests were carried out following the method NBR 9778 [40].



## 2.6 Eco-efficiency performance

The eco-efficiency performance of the LWASCMs was determined by the Binder Intensity (*BI*) indicator, proposed by Damineli et al. [41] and calculated by Equation 3, where the total consumption of binder (*b*) and the performance achieved in the compressive strength test at 28 days (*p*) were the input parameters.

$$BI = \frac{b}{p} \tag{3}$$

## 2.7 Statistical analysis

Response surfaces were drawn for compressive strength, tensile strength, void ratio, density, ultrasonic pulse velocity, water volume, and binder intensity to optimize the experimental design. A regression equation was found for each test performed that estimates the expected values for different proportions of *f/c* and  $V_{LWA}/V_{CA}$  based on the results obtained from the tests (Equation 4) [19]. The coefficients of determination ( $R^2$ ) were found to verify the fit of the regression equations obtained for a significance p-value lower than 0.05. The closer the  $R^2$  value to 1, the better the fit.

$$y = \beta_0 + \beta_1 a_i + \beta_2 a_i^2 + \beta_3 b_j + \beta_4 b_j^2 + \beta_5 a_i b_j + \varepsilon_{ij} \tag{4}$$

## 3 RESULTS AND DISCUSSIONS

### 3.1 Fresh microconcrete properties

According to the plastic viscosity tests presented in Table 6, the increase in the OSW content leads to a decrease in the viscosity of the paste. Therefore, mixtures with higher contents of OSW demand a lower water/powder ratio to maintain workability without tendency to segregate LWA [6]. The spreading of the produced mixtures that reached the 260 to 280 mm range in Figure 6 showed stable mixtures, not presenting signs of segregation and with homogeneous LWA distribution. However, as we will see later, this observation is not enough to guarantee that the EPS lightweight aggregate will present a uniform distribution along the height of the specimens.

**Table 6.** Viscosity of the fluid pastes measured by the Fann 35A rotational viscometer.

| filler/cement ( <i>f/c</i> ) | 0  | 1  | 2  |
|------------------------------|----|----|----|
| Plastic viscosity (mPa·s)    | 73 | 72 | 59 |

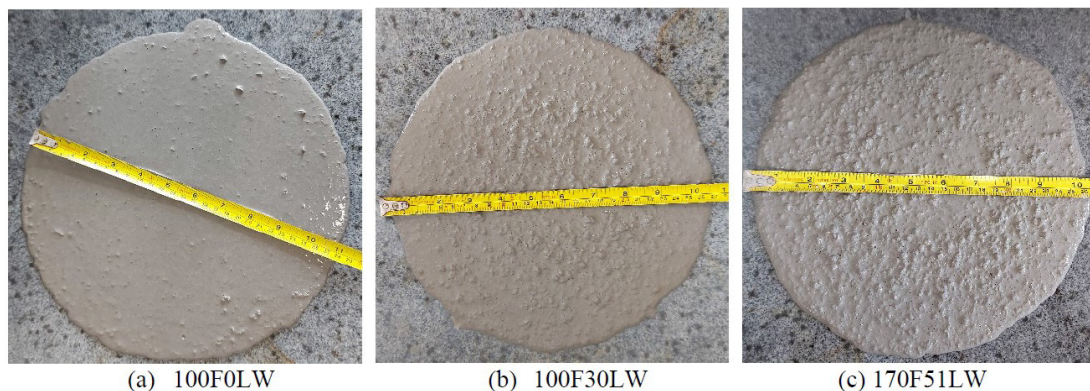


**Figure 6.** Mini slump spreading of LWASCM: (a) 100F0LW; (b) 100F30LW; (c) 170F51LW.

The water-to-powder volume ratio ( $V_w/V_p$ ) of each mixture, mini-slump spreading, mini-slump correlation with slump flow, and  $T_{220}$  values are presented in Table 7. The coded regression equation of the water consumption and contour graphs are shown in Table 8 and Figure 7, respectively.

**Table 7.** Test results.

| Mixture   | $V_w/V_p$ | Mini-Slump (mm) | Correlation Slump Flow (mm) | $T_{220}$ (s) | Compressive strength at 28 days (MPa) | Tensile strength in diametrical compression at 28 days (MPa) | Ultrasonic pulse velocity at 28 days (m/s) | Density (g/cm <sup>3</sup> ) | Void Index (%) | Binder intensity (bi) |
|-----------|-----------|-----------------|-----------------------------|---------------|---------------------------------------|--|--|------------------------------|----------------|-----------------------|
| 100F0LWA  | 0.874     | 280             | 615                         | 3.91          | 41.42                                 | 4.21   | 3856                                       | 2.66                         | 21.9           | 11.16                 |
| 170F9LWA  | 0.936     | 275             | 604                         | 3.12          | 16.72                                 | 2.85   | 3545                                       | 2.51                         | 24.3           | 20.06                 |
| 29F9LWA   | 1.092     | 265             | 582                         | 5.13          | 37.53                                 | 4.35   | 3847                                       | 2.46                         | 20.3           | 17.90                 |
| 0F30LWA   | 1.248     | 265             | 582                         | 2.10          | 17.45                                 | 4.03   | 3677                                       | 2.36                         | 19.5           | 47.70                 |
| 100F30LWA | 0.967     | 270             | 593                         | 2.98          | 17.06                                 | 2.95   | 3524                                       | 2.38                         | 22.7           | 26.37                 |
| 200F30LWA | 0.780     | 280             | 615                         | 3.00          | 7.18                                  | 1.97   | 3286                                       | 2.35                         | 21.6           | 44.15                 |
| 170F51LWA | 0.905     | 270             | 593                         | 4.22          | 12.39                                 | 2.18   | 3420                                       | 2.21                         | 23.2           | 27.31                 |
| 29F51LWA  | 1.123     | 273             | 600                         | 2.23          | 9.30                                  | 2.92   | 3417                                       | 2.24                         | 23.6           | 71.60                 |
| 100F60LWA | 0.874     | 260             | 571                         | 5.34          | 12.39                                 | 2.18   | 3420                                       | 2.21                         | 23.2           | 37.31                 |

**Table 8.** Coded regression equations of the results.

| Regression equations   | $\epsilon$ , std.dev. | R <sup>2</sup> /R <sup>2</sup> aj |
|--|-----------------------|-----------------------------------|
| $\frac{V_w}{V_p} = 0.9247 - 0.0827 \frac{f}{c} - 0.0468 \frac{V_{LWA}}{V_{CA}} + 0.0596 \left(\frac{f}{c}\right)^2$  | 0.1057                | 51.15%/ 44.78%                    |
| $f_c \text{ (MPa)} = 11.035 - 4.590 \frac{f}{c} - 9.761 \frac{V_{LWA}}{V_{CA}} + 7.567 \left(\frac{V_{LWA}}{V_{CA}}\right)^2 + 4.854 \frac{V_{LWA}}{V_{CA}} \cdot \frac{f}{c}$   | 1.7273                | 98.35%/ 98.05%                    |
| $\text{Tensile strenght (MPa)} = 2.8926 - 0.7064 \frac{f}{c} - 0.6867 \frac{V_{LWA}}{V_{CA}} + 0.1185 \left(\frac{V_{LWA}}{V_{CA}}\right)^2$   | 0.1752                | 97.08%/ 96.70%                    |
| $\text{UPV (MPa)} = 3473.7 - 128.1 \frac{f}{c} - 168.3 \frac{V_{LWA}}{V_{CA}} + 68.1 \left(\frac{V_{LWA}}{V_{CA}}\right)^2$  | 92.7483               | 85.22%/ 83.30%                    |
| $\text{Density (kg/m}^3\text{)} = 2.41886 - 0.005 \frac{f}{c} - 0.15614 \frac{V_{LWA}}{V_{CA}} - 0.04032 \left(\frac{f}{c}\right)^2 + 0.01019 \left(\frac{V_{LWA}}{V_{CA}}\right)^2$                                   | 0.0086                | 99.74%/ 99.69%                    |
| $\text{Void Index (\%)} = 24.722 + 0.674 \frac{f}{c} + 0.369 \frac{V_{LWA}}{V_{CA}} - 1.825 \left(\frac{f}{c}\right)^2 - 0.822 \left(\frac{V_{LWA}}{V_{CA}}\right)^2 - 1.377 \frac{V_{LWA}}{V_{CA}} \cdot \frac{f}{c}$ | 0.6228                | 89.26%/ 86.71%                    |
| $\text{BI} = 46.98 - 3.99 \frac{f}{c} + 14.31 \frac{V_{LWA}}{V_{CA}} - 10.44 \left(\frac{V_{LWA}}{V_{CA}}\right)^2 - 7.81 \frac{V_{LWA}}{V_{CA}} \cdot \frac{f}{c}$  | 6.9461                | 87.78%/ 85.56%                    |

$\frac{V_w}{V_p}$  - water-to-powder volume ratio;  $f_c$  - compressive strength; UPV - ultrasonic pulse velocity; BI - Binder Intensity.

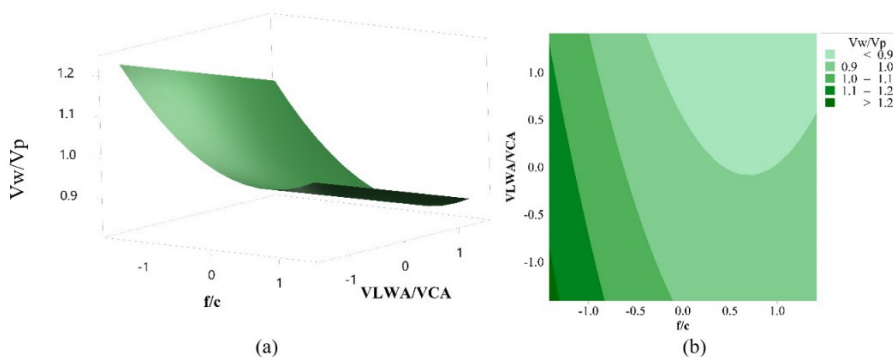


**Figure 7.** Plots of coded (a) surface and (b) contour of the water-to-powder volume ratios ( $V_w/V_p$ ).



The results of  $V_w/V_p$  in Figure 7 show that the increase in the powder content considerably reduced the water necessary for the mixture to reach the fixed spread, which is the most significant variable and agrees with the results of plastic viscosity [42], [43]. The increase in the content of lightweight aggregates also decreased water consumption, which may be due to the smooth water-repellent particles of LWA, increasing the fluidity of the mixture, as observed by other researchers [8], [44]–[46]. However, the  $R^2$  of the regression equation, even after adjusting the terms, showed low significance, and therefore, despite representing the rheological behavior of the materials, the equation may not lead to accurate results.

In the preliminary tests, higher water consumption for mixtures with high LWA content led to segregation and flotation of the aggregates. Lower water must be used to achieve cohesive mixtures without the risk of segregation in the LWASCM, and the spreading must be controlled by increasing the consumption of superplasticizer and OSW filler.

### 3.2 Hardened concrete properties

Tables 7 and 8 show the compressive and tensile strength results with their well-adjusted regression equations. Compressive strength is mainly governed by  $V_w/V_p$ , demonstrating that this is the most significant factor, and the higher its value, the lower the mechanical strength obtained. The tensile strength in diametrical compression has both factors as predominant, reduced by increased consumption of LWA and by replacing cement with filler. This difference in the significance of the terms in the two mechanical strength tests can be explained by Figure 8, which shows the images of the broken specimens obtained in the diametrical compression test of each mixture.



**Figure 8.** Images of the broken specimens obtained in the diametrical compression tests.

It can be seen from Figure 8 that the higher the content of LWA, the greater the segregation of the aggregates, making it easy to visually observe the difference in the concentration of LWA at the height of the specimen. Images a, b and c of Figure 7 are the only ones that do not show segregation and are from the mixtures 100F0LWA, 170F5LWA and 29F9LWA with a low proportion of LWA, which, when analyzed in their mechanical strength results, present the highest strengths, falling only due to the high consumption of inert material in the 170F9LWA mixture.

On the other hand, the specimens shown in images d, e, f, g, h, and i of Figure 8, for having higher levels of LWA, showed strong segregation by flotation of LWA, which was not properly anticipated by the spread test. The high concentration of LWA on top of the specimens created a disproportionate lightweight layer with low paste concentration and, consequently, low mechanical strength, inducing the rupture in the compression test in these layers, maintaining the rest of the specimen intact (Figure 9).



**Figure 9.** Specimen ruptured in the compressive strength test.

The 100F60LWA mix suffered a 70% drop in mechanical strength compared to the 100F0LWA mix, with the maximum substitution of conventional aggregate for lightweight aggregate. The high drop in mechanical strength is similar to the results of Rosca and Corobceanu [47], who replaced aggregates in volume by up to 35% and had a drop of up to 66% in the mechanical strength of concrete. Mohammed and Aayeel [46] also replaced coarse aggregates with EPS in volume by up to 60% and had a drop of up to 80% in the compressive strength and 40% in the tensile strength of concrete.

The tensile strength by diametral compression test is performed by applying a force along the length of the specimen, and, therefore, part of the force is applied in the compact layers with lower concentrations of LWA, inducing unrealistic higher results.

While in the compressive strength test, the LWA-rich layer governed the results making  $V_{LWA}/V_{CA}$  artificially having greater significance, in the tensile strength test, the entire specimen influenced the results, and therefore, both  $V_{LWA}/V_{CA}$  and  $f/c$  were significant. The surface and contour plots in Figure 9 illustrate the mixtures' mechanical strength drop according to the increase in OSW and LWA contents.

The ultrasonic pulse velocity results are similar to the tensile strength results, which are also strongly influenced by the disproportionate layers. However, for UPV, the consumption of LWA is more important in the results, decreasing the speeds with the increase of LWA.

Despite the segregation, lack of stability of the matrix, and the consequent high drop in mechanical strength, the incorporation of LWA managed to reduce the density of the microconcretes. According to Table 7, the mixture with the highest content of LWA, 100F60LWA, reached 2.21 g/cm<sup>3</sup>, a density 17% lower than that of the mix 100F0LWA, with a reduction of 450 kg/m<sup>3</sup>. However, the lowest density found is insufficient to classify this microconcrete as lightweight. Nevertheless, it is important to mention that the proportion of aggregate in self-compacting microconcretes is considerably reduced compared to conventional concrete, reducing the margin for reducing mass by partially replacing sand with lightweight aggregates.

The density regression equation was adjusted, with R<sup>2</sup> close to 1 and with the term  $V_{LWA}/V_{CA}$  with greater significance, demonstrating that the incorporation of LWA has a direct connection with the drop in the mixtures' density can also be observed in the graphs in Figure 10.

The void ratio in mixtures with  $V_{LWA}/V_{CA}$  up to 0.09 increased with increasing filler content, making  $f/c$  more significant in the regression equations. However, in mixtures with replacements of conventional aggregates by LWA above 30%, the floatation of LWA interfered with the readings, causing LWASCM with similar proportions of LWA to have similar void ratios, regardless of the concentration of  $f/c$ .

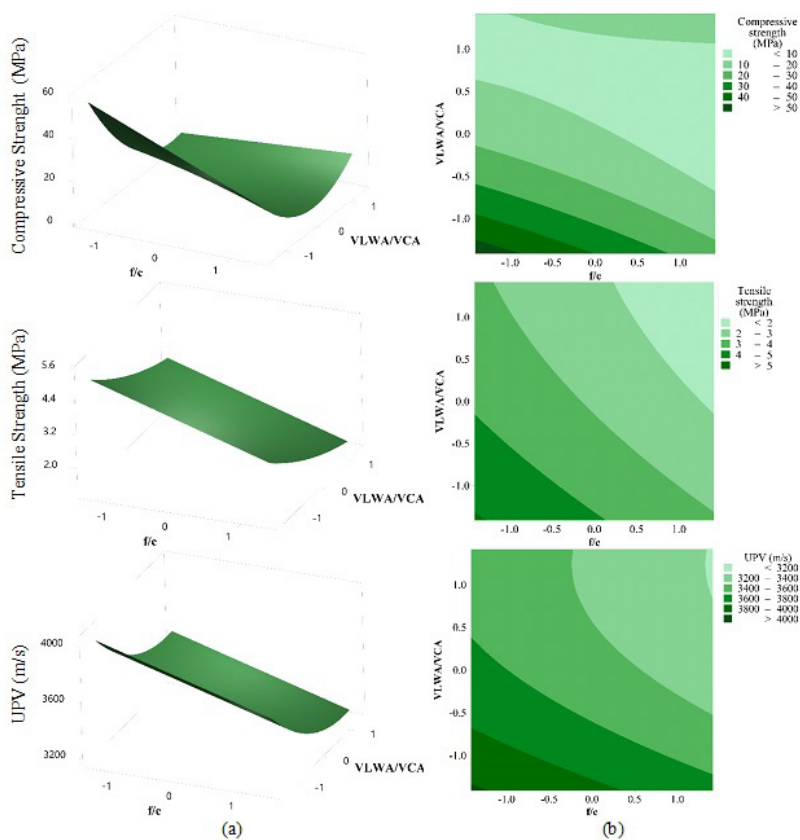


**Figure 10.** Plots of (a) surface and (b) contour of compressive strength, tensile strength and UPV.

Figure 11 shows a convex surface in which  $f/c$  up to 1 and  $V_{LWA}/V_{CA}$  from up to 0.3 increase the void ratio, and mixtures with these two parameters above these values present lower void ratios. This result may be linked to the difference in water consumption, in which, despite the increase in  $f/c$  increasing the void ratio, the filler provides better spreading, requiring a lower  $V_w/V_p$ , which reduces the voids left by the water. The 100F60LWA mixture, despite having the maximum concentration of LWA, presented the lightweight aggregates less concentrated at the top and better distributed along with the specimen, i.e., the mixture was more cohesive and less prone to segregation, which may be due to a reduction in the water consumption and increase in the filler content. On the other hand, despite the drop in water consumption, the void ratio did not decrease with increasing LWA, demonstrating that LWA can lead to increased absorption and void ratio in concrete [44].



Therefore, although the results demonstrate that the increase in  $f/c$  and  $V_{LWA}/V_{CA}$  decreased the mechanical strength and density and increased the void ratio of the lightweight microconcretes, the segregation of LWA did not allow the results to demonstrate the real mechanical potential of these microconcretes.

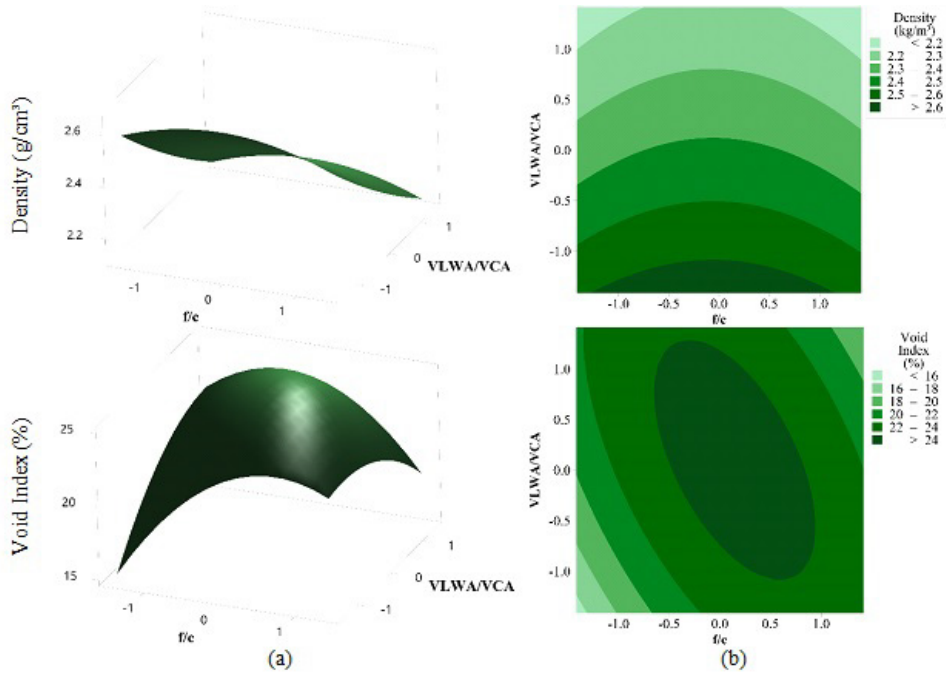


Figure 11. Adjusted graphs of (a) surface and (b) contour for density and void index.

### 3.3 Eco-efficiency performance

Figure 12 shows the graphs of Binder Intensity (BI). Although the increase in the filler content decreased the  $BI$  in mixtures containing LWA and increased eco-efficiency through the high incorporation of waste and reduction of cement, the LWA is significant and considerably increased the  $BI$ , decreasing eco-efficiency.

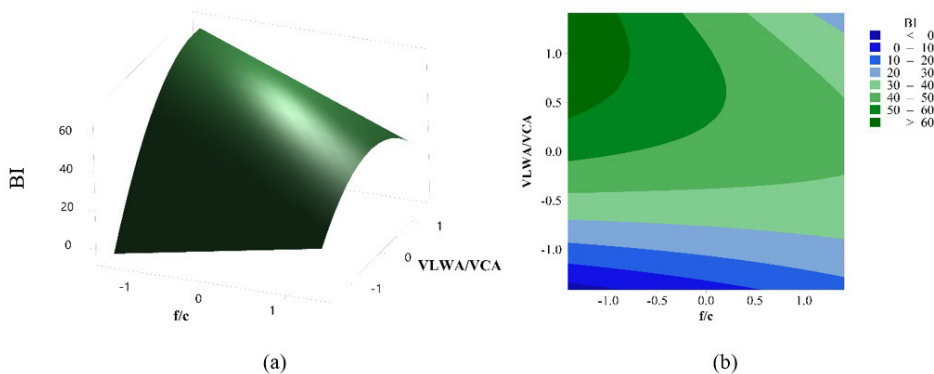


Figure 12. Adjusted graphs of (a) surface and (b) contour for Binder Intensity (BI).

The results were already expected since the indicator only considers cement consumption and mechanical strength, i.e., mixtures with lower cement consumption and high strengths have better eco-efficiency performances according to this indicator. Therefore, the waste reuse and reduction of primary raw materials also are significant eco-efficiency indicators but not considered in this study. For this reason, these parameters controversially figured as eco-efficiency reducers.

As lightweight concretes generally have lower mechanical strengths in relation to cement consumption, it was expected that mixtures with LWA would have higher  $BI$ . However, the high  $BI$  (above 20) indicates that the segregation of LWA and the consequent drop in mechanical strength diverged the results, causing the mixtures that did not segregate to present an increased  $BI$  with the increase of the filler content. In contrast, the mixtures that segregated had lower  $BI$  for lower cement consumption, and the increase in the  $f/c$  ratio increased eco-efficiency as they had similar mechanical strengths.

Therefore, matrix stabilization by increasing resistance to segregation must be provided for adjusted results. Other sustainability indicators must be considered for a more consistent eco-efficiency performance evaluation of LWASCM containing inert waste.

#### 4 CONCLUSIONS

The present work studied the production of lightweight aggregate self-compacting microconcretes with partial replacement of cement by Ornamental Stone Waste filler and partial replacement of conventional aggregate by lightweight aggregate obtained from Expanded Polystyrene Waste.

The mixtures with  $V_{LWA}/V_{CA}$  above 0.3 evidenced the difficulty of stabilizing the mixtures by the remarkable small density of the EPS, causing drop in mechanical strength and void ratio and generating results with important distortions. However, despite the floatation of the aggregates, the increase in  $f/c$  and  $V_{LWA}/V_{CA}$  led to a decrease in the consumption of water for a fluid mixture. The increase in  $V_{LWA}/V_{CA}$  also decreased the density of the mixtures, making the microconcretes lighter.

The interaction of ornamental stone filler with the lightweight aggregate proved promising in improving the eco-efficiency of the lightweight microconcretes. The increase in  $f/c$  decreased the binder intensity, as the reduction in cement consumption did not lead to a drop in strength in the same proportion.

Strategies for stabilizing mixtures with lightweight aggregates such as reducing the spreading range to reduce water consumption and segregation, or reducing water consumption by increasing the superplasticizer content and adding mineral additions to increase the shear stress are proposed to extend the present study, avoiding the observed distortions and providing a deeper evaluation of the influence of the tested parameters.

#### ACKNOWLEDGEMENTS

The authors are grateful to the Research Group SICon-CNPq/UFV and the partner groups from the Rede Mineira de Pesquisa, desenvolvimento científico, tecnológico e inovação for providing infrastructure and valuable technical assistance and academic support. The authors would like to acknowledge the Nucleus of Microscopy and Microanalysis at the Universidade Federal de Viçosa, (<http://www.nmm.ufv.br/>) for providing the equipment and technical support for experiments involving electron microscopy.

#### REFERENCES

- [1] J. A. Rossignolo, *Concreto Leve Estrutural: Produção, Propriedades, Microestrutura e Aplicações*. São Paulo, Brazil: PINI, 2009.
- [2] A. S. Souza and C. M. Carvalho, "Low density self compacting concrete: for application in pre-fabricated panels," *Rev. InterScientia*, vol. 5, pp. 75–91, Dec. 2017.
- [3] B. Vakhshouri and S. Nejadi, "Mix design of light-weight self-compacting concrete," *Case Stud. Constr. Mater.*, vol. 4, pp. 1–14, Jun. 2016, <http://dx.doi.org/10.1016/j.cscm.2015.10.002>.
- [4] A. F. Angelin, R. C. C. Lintz, W. R. Osório, and L. A. Gachet, "Evaluation of efficiency factor of a self-compacting lightweight concrete with rubber and expanded clay contents," *Constr. Build. Mater.*, vol. 257, pp. 119573, Oct. 2020, <http://dx.doi.org/10.1016/j.conbuildmat.2020.119573>.
- [5] N. N. Hilal, M. F. Sahab, and T. K. M. Ali, "Fresh and hardened properties of lightweight self-compacting concrete containing walnut shells as coarse aggregate," *J. King Saud Univ. Eng. Sci.*, vol. 33, no. 5, pp. 364–372, Jul. 2021, <http://dx.doi.org/10.1016/j.jksues.2020.01.002>.
- [6] D. S. L. Y. Wan, F. Aslani, and G. Ma, "Lightweight self-compacting concrete incorporating perlite, scoria, and polystyrene aggregates," *J. Mater. Civ. Eng.*, vol. 30, no. 8, pp. 04018178, May 2018, [http://dx.doi.org/10.1061/\(asce\)mt.1943-5533.0002350](http://dx.doi.org/10.1061/(asce)mt.1943-5533.0002350).
- [7] R. Madandoust, M. M. Ranjbar, and S. Y. Mousavi, "An investigation on the fresh properties of self-compacted lightweight concrete containing expanded polystyrene," *Constr. Build. Mater.*, vol. 25, no. 9, pp. 3721–3731, Sep. 2011, <http://dx.doi.org/10.1016/j.conbuildmat.2011.04.018>.
- [8] M. M. Ranjbar and S. Y. Mousavi, "Strength and durability assessment of self-compacted lightweight concrete containing expanded polystyrene," *Mater. Struct. Constr.*, vol. 48, no. 4, pp. 1001–1011, Nov. 2015, <http://dx.doi.org/10.1617/s11527-013-0210-6>.

- [9] S. Yang, X. Yue, X. Liu, and Y. Tong, "Properties of self-compacting lightweight concrete containing recycled plastic particles," *Constr. Build. Mater.*, vol. 84, pp. 444–453, Jun. 2015, <http://dx.doi.org/10.1016/j.conbuildmat.2015.03.038>.
- [10] G. E. Abdelaziz, "A study on the performance of lightweight self-consolidated concrete," *Mag. Concr. Res.*, vol. 62, no. 1, pp. 39–49, Jan. 2010, <http://dx.doi.org/10.1680/macrc.2008.62.1.39>.
- [11] J. Li, Y. Chen, and C. Wan, "A mix-design method for lightweight aggregate self-compacting concrete based on packing and mortar film thickness theories," *Constr. Build. Mater.*, vol. 157, pp. 621–634, Dec. 2017, <http://dx.doi.org/10.1016/j.conbuildmat.2017.09.141>.
- [12] Z. S. Ali, M. Hosseinpour, and A. Yahia, "New aggregate grading models for low-binder self-consolidating and semi-self-consolidating concrete (Eco-SCC and Eco-semi-SCC)," *Constr. Build. Mater.*, vol. 265, pp. 120314, Dec. 2020, <http://dx.doi.org/10.1016/j.conbuildmat.2020.120314>.
- [13] R. M. Andrew, "Global CO<sub>2</sub> emissions from cement production, 1928–2018," *Earth Syst. Sci. Data*, vol. 11, no. 4, pp. 1675–1710, Nov. 2019, <http://dx.doi.org/10.5194/essd-11-1675-2019>.
- [14] S. Çankaya and B. Pekey, "A comparative life cycle assessment for sustainable cement production in Turkey," *J. Environ. Manage.*, vol. 249, pp. 109362, Dec. 2019, <http://dx.doi.org/10.1016/j.jenvman.2019.109362>.
- [15] N. Gupta, R. Siddique, and R. Belarbi, "Sustainable and greener self-compacting concrete incorporating industrial by-products: a review," *J. Clean. Prod.*, vol. 284, pp. 124803, Feb. 2020, <http://dx.doi.org/10.1016/j.jclepro.2020.124803>.
- [16] J. Lehne and F. Preston, *Making Concrete Change – Innovation in Low-Carbon Cement and Concrete*. London, United Kingdom: Chatam House, 2018.
- [17] P. K. Mehta and P. J. M. Monteiro, *Concreto: Propriedades e Materiais*. São Paulo, Brazil: IBRACON, 2014.
- [18] E. Worrell, L. Price, N. Martin, C. Hendriks, and L. O. Meida, "Carbon dioxide emissions from the global cement industry," *Annu. Rev. Energy Environ.*, vol. 26, no. 1, pp. 303–329, Nov. 2001, <http://dx.doi.org/10.1146/annurev.energy.26.1.303>.
- [19] A. M. Souza, J. M. F. Carvalho, C. F. R. Santos, F. A. Ferreira, L. G. Pedroti, and R. A. F. Peixoto, "On the strategies to improve the eco-efficiency of self-compacting concrete using industrial waste: an analytical review," *Constr. Build. Mater.*, vol. 347, pp. 128634, Sep. 2022, <http://dx.doi.org/10.1016/j.conbuildmat.2022.128634>.
- [20] EFNARC, *The European Guidelines for Self-Compacting Concrete*, 2005. Accessed: Dec. 22, 2023. [Online]. Available: <https://efnarc.org/publications>
- [21] P. C. C. Gomes and A. R. Barros, *Métodos de Dosagem de Concreto Autoadensável*. São Paulo, Brazil: PINI, 2009.
- [22] A. M. Neville, *Propriedades do concreto*. Porto Alegre, Brasil: Bookman, 2016.
- [23] H. Okamura and M. Ouchi, "Self-compacting concrete," *J. Adv. Concr. Technol.*, vol. 1, no. 1, pp. 5–15, Apr. 2003.
- [24] Associação Brasileira da Indústria de Rochas Ornamentais, *Balanco das Exportações e Importações Brasileiras de Rochas Ornamentais em 2019*. Brasília, Brazil: ABIROCHAS, 2020.
- [25] E. Bacarji, R. D. Toledo Fo., E. A. B. Koenders, E. P. Figueiredo, and J. L. M. P. Lopes, "Sustainability perspective of marble and granite residues as concrete fillers," *Constr. Build. Mater.*, vol. 45, pp. 1–10, Aug. 2013, <http://dx.doi.org/10.1016/j.conbuildmat.2013.03.032>.
- [26] M. A. Rodrigues and J. A. Melo Fo., "Fabricação de concreto autoadensável com utilização de resíduos de marmorarias como adição mineral," *Rev. Eletrônica Eng. Civil*, vol. 14, pp. 50–71, Jan. 2017.
- [27] M. S. Zafar, U. Javed, R. A. Khushnood, A. Nawaz, and T. Zafar, "Sustainable incorporation of waste granite dust as partial replacement of sand in autoclave aerated concrete," *Constr. Build. Mater.*, vol. 250, pp. 118878, Jul. 2020, <http://dx.doi.org/10.1016/j.conbuildmat.2020.118878>.
- [28] R. Alyousef, O. Benjeddou, C. Soussi, M. A. Khadimallah, and M. Jedidi, "Experimental study of new insulation lightweight concrete block floor based on perlite aggregate, natural sand, and sand obtained from marble waste," *Adv. Mater. Sci. Eng.*, vol. 2019, pp. 8160461, Mar. 2019, <http://dx.doi.org/10.1155/2019/8160461>.
- [29] J. E. Funk and D. R. Dinger, "Particle size control for high-solids castable refractories," *Am. Ceram. Soc. Bull.*, vol. 73, no. 10, pp. 68–72, Oct. 1994.
- [30] A. L. Castro and V. C. Pandolfelli, "Revisão: conceitos de dispersão e empacotamento de partículas para a produção de concretos especiais aplicados na construção civil," *Cerâmica*, vol. 55, no. 333, pp. 18–32, Mar. 2009, <http://dx.doi.org/10.1590/s0366-69132009000100003>.
- [31] F. T. Ramal Jr., R. G. Pileggi, J. B. Gallo, and V. C. Pandolfelli, "A curva de distribuição granulométrica e sua influência na reologia de concretos refratários," *Cerâmica*, vol. 48, no. 308, pp. 212–216, Dec. 2002, <http://dx.doi.org/10.1590/s0366-69132002000400008>.
- [32] R. Sarkar, "Particle size distribution for refractory castables: a review," *Int. Ceram. Rev.*, vol. 65, no. 3, pp. 82–86, Jun. 2016, <http://dx.doi.org/10.1007/bf03401156>.
- [33] R. Vanderlei, "Análise experimental do concreto de pós reativos: dosagem e propriedades mecânicas," Doctoral dissertation, Esc. Eng. São Carlos, Univ. São Paulo, São Carlos, Brazil, 2004.



- [34] K. Liu, T. Yin, D. Fan, J. Wang, and R. Yu, "Multiple effects of particle size distribution modulus ( $q$ ) and maximum aggregate size ( $D_{max}$ ) on the characteristics of Ultra-High Performance concrete (UHPC): experiments and modeling," *Cement Concr. Compos.*, vol. 133, pp. 104709, Oct. 2022, <http://dx.doi.org/10.1016/j.cemconcomp.2022.104709>.
- [35] Associação Brasileira de Normas Técnicas, *Concreto e Argamassa – Determinação da Resistência à Tração por Compressão Diametral de Corpos de Prova Cilíndricos*, NBR 7222, 2011.
- [36] Associação Brasileira de Normas Técnicas, *Concreto – Ensaio de Compressão de Corpos de Prova Cilíndricos*, NBR 5739, 2018.
- [37] ASTM International, *Standard Test Method for Compressive Strength of Cylindrical Concrete Specimens*, ASTM C39/C39M, 2010. <http://dx.doi.org/10.1520/C0039>.
- [38] Associação Brasileira de Normas Técnicas, *Concreto Endurecido – Determinação da Velocidade de Propagação de Onda Ultrassônica*, NBR 8802, 2019.
- [39] ASTM International, *Standard Test Method for Pulse Velocity Through Concrete*, C597-16, 2016.
- [40] Associação Brasileira de Normas Técnicas, *Argamassa e Concreto Endurecidos – Determinação da Absorção de Água, Índice de Vazios e Massa Específica*, NBR 9778, 2011.
- [41] B. L. Damineli, F. M. Kemeid, P. S. Aguiar, and V. M. John, "Measuring the eco-efficiency of cement use," *Cement Concr. Compos.*, vol. 32, no. 8, pp. 555–562, Sep. 2010, <http://dx.doi.org/10.1016/j.cemconcomp.2010.07.009>.
- [42] B. C. Xavier et al., "Fresh and hardened states of distinctive self-compacting concrete with marble- and phyllite-powder aggregate contents," *J. Mater. Civ. Eng.*, vol. 32, no. 5, pp. 04020065, Feb. 2020, [http://dx.doi.org/10.1061/\(asce\)mt.1943-5533.0003103](http://dx.doi.org/10.1061/(asce)mt.1943-5533.0003103).
- [43] D. M. Sadek, M. M. El-Attar, and H. A. Ali, "Reusing of marble and granite powders in self-compacting concrete for sustainable development," *J. Clean. Prod.*, vol. 121, pp. 19–32, May 2016, <http://dx.doi.org/10.1016/j.jclepro.2016.02.044>.
- [44] S. K. Adhikary and D. K. Ashish, "Turning waste expanded polystyrene into lightweight aggregate: towards sustainable construction industry," *Sci. Total Environ.*, vol. 837, pp. 155852, Sep. 2022, <http://dx.doi.org/10.1016/j.scitotenv.2022.155852>.
- [45] C. H. R. Carvalho and L. A. C. Motta, "Study about concrete with recycled expanded polystyrene," *Rev. IBRACON Estrut. Mater.*, vol. 12, no. 6, pp. 1390–1407, Nov./Dec. 2019, <http://dx.doi.org/10.1590/s1983-41952019000600010>.
- [46] H. J. Mohammed and O. K. Aayeel, "Flexural behavior of reinforced concrete beams containing recycled expandable polystyrene particles," *J. Build. Eng.*, vol. 32, pp. 101805, Sep. 2020, <http://dx.doi.org/10.1016/j.jobbe.2020.101805>.
- [47] B. Rosca and V. Corobceanu, "Structural grade concrete containing expanded polystyrene beads with different particle distributions of normal weight aggregate," *Mater. Today Proc.*, vol. 42, pp. 548–554, Nov. 2020, <http://dx.doi.org/10.1016/j.matpr.2020.10.517>.

---

**Author contributions:** AMS: conceptualization, data curation, formal analysis, methodology, writing; JMFC: funding acquisition, supervision, formal analysis, writing; CFRS: writing, conceptualization, formal analysis; FAF: writing, conceptualization, formal analysis; LGP: writing, conceptualization, formal analysis; RAFP: writing, supervision, formal analysis.

**Editors:** Alexander Mark, Daniel Carlos Taissum Cardoso.